

Near-field Evaluation of Artificial Upwelling Concepts for Open-ocean Oligotrophic Conditions

GÉRARD C. NIHOUS*

Hawaii Natural Energy Institute, University of Hawaii, 1680 East-West Road, POST 109, Honolulu, Hawaii 96822, USA

The near-field behavior of artificially upwelled deep nutrient-rich water is characterized for open-ocean oligotrophic conditions. Two basic concepts are considered: the near-surface release of negatively buoyant plumes, or the direct mixing of deep and surface waters in a prescribed ratio. As expected, direct mixing would be more effective in vertically stabilizing a given water mixture. Because of a deep quasi-permanent thermocline, however, direct mixing would require considerably greater dilution in tropical open-ocean waters than was necessary during a recent summertime test in Sagami Bay, Japan: the concept might be limited to very small deep water flow rates. A brief consideration of Gross Primary Production in oligotrophic waters confirms that phytoplankton is well adapted to nanomolar nitrate concentrations. Hence, a modest dilution of artificially upwelled nutrients may not be detrimental in boosting primary productivity. This is shown when considering plumes released in a small crossflow (instead of a 'stagnant' water column): the relative benefit of shallower vertical stabilization appears to exceed the relative drawback of greater dilution. In those cases, it is suggested that deep seawater flow rates higher than 10 to 20 m³/s may not provide much additional enhancement.

Keywords: deep-ocean water, nutrients, gross primary production, artificial upwelling

INTRODUCTION

As the 21st Century started, fisheries worldwide have been facing declining stocks and an uncertain future in a changing global environment. Yet, much of the fish catch still occurs in very small oceanic regions of upwelling. Upwelled waters are rich in nutrients essential for biological activity, and when exposed to sufficient sunlight near the ocean surface, phytoplankton growth is promoted to the benefit of the entire food web. When seawater is stratified from density differences, however, biological activity is limited by the availability of nutrients in a relatively shallow photic layer: deep-water nutrients essentially remain out of reach throughout vast oceanic regions.

For the past half century at least, the possibility of man-made Artificial Upwelling

*Corresponding author: nihous@hawaii.edu

(AU) has been evoked in the scientific and technical literature (e.g. Stommel et al., 1956). From the seventies, great strides in ocean engineering prompted by offshore oil exploitation, and a regained interest in renewable technologies requiring deep seawater, like Ocean Thermal Energy Conversion (OTEC), have sustained some enthusiasm for AU technologies. Simple as the idea may be, however, it has not been practically implemented. The relative lack of success of some serious ventures to investigate the concept at sea (like the landmark Toyama Bay project in the mid nineties; Kajikawa, 1997) could represent a warning that 'the natural world (thermocline) is not easily turned upside down'.

A new program in Japan has once more called the attention of the AU community with very promising results reported from a recent at-sea test (Ouchi and Ohmura, 2004). The TAKUMI concept is presented as a means to more directly control the dilution and location of nutrient-rich upwelled waters by avoiding typical plume dynamics. Instead of relying on the gravitational settling and mixing of a plume of denser nutrient-rich water, the proponents of the TAKUMI concept call for directly mixing 'heavy' and 'light' waters in a specifically designed system.

This paper will examine traditional AU plumes as well as the TAKUMI idea in the context of real ocean data collected for the Hawaii Ocean Time-series (HOT) program. Observations of the hydrography, chemistry and biology of the water column have been made since October 1988 at the deep-water Station ALOHA (A Long-term Oligotrophic Habitat Assessment; 22° 45' N, 158° 00' W) 100 km north of Oahu, Hawaii (Karl and Lukas, 1996; http://hahana.soest.hawaii.edu/hot/hot_jgofs.html). The data provides a

comprehensive description of the ocean at a site representative of the oligotrophic North Pacific Subtropical Gyre. Reports have been released every year; the latest (13th) is by Fujieki et al. (2004), and many research articles based on the HOT program have already been published (e.g. Siegel et al., 2001). The complete data set is readily accessible through the internet-based Hawaii Ocean Time-series Data Organization and Graphical System (<http://hahana.soest.hawaii.edu/hot/hot-dogs/interface.html>).

The challenge of vertically stabilizing heavier water in the surface layer of a stratified water column will first be re-examined. Simple specific characteristics of primary productivity in oligotrophic environments will then be reviewed before attempting an evaluation of the near-field performance of AU strategies.

VERTICAL STABILIZATION OF UPWELLED NUTRIENT-RICH DEEP WATER

The most challenging problem faced by proponents of 'artificial upwelling' is to vertically stabilize the heavier nutrient-rich deep water within the photic layer without excessive dilution. There has recently been an ambitious program in Japan where the mixing of some deep water with surface water is directly promoted by a double pump system, the so-called TAKUMI concept. It was successfully tested in Sagami Bay (Ouchi and Ohmura, 2004), where a nutrient-rich mixture was generated and stabilized no deeper than about 20 m below the surface with a low mixing ratio of the order of two-to-one (in our plume terminology, an absolute dilution *S* of three). Vertical stabilization otherwise relies on releasing the deep water into the surface layer, where it

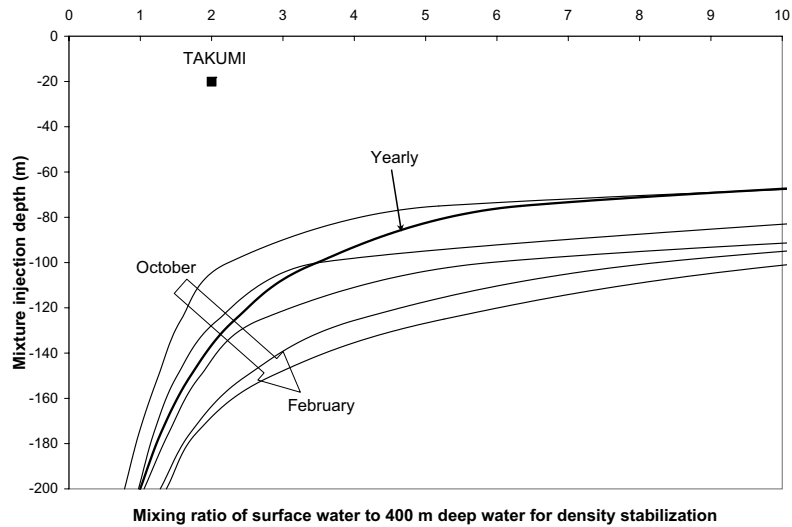


FIGURE 1
Illustration of the TAKUMI concept at ALOHA Station with data from October through February.

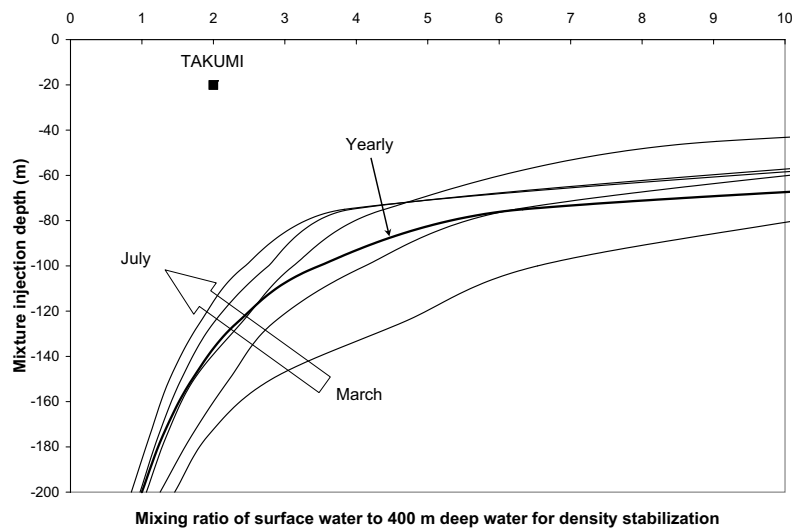


FIGURE 2
Illustration of the TAKUMI concept at ALOHA Station with data from March through July.

evolves as a negatively buoyant plume²; owing to the ambient density stratification, this plume eventually settles to a neutral-

buoyancy depth through turbulent mixing. These strategies will be reviewed for realistic open-ocean oligotrophic conditions.

²The initial (negative) buoyancy flux of proposed AU systems is large enough that mass and momentum effects on the mixing of the released water would be limited in magnitude and confined to a small region. Hence, only 'plumes' have been considered in this evaluation.

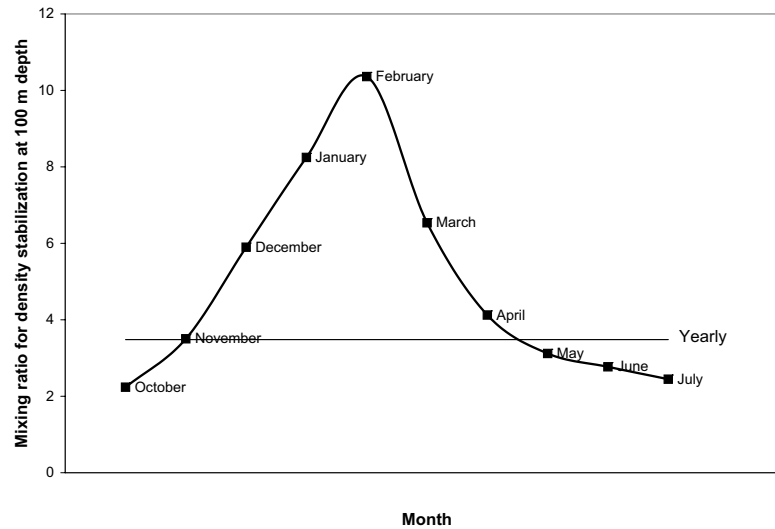


FIGURE 3
Illustration of the TAKUMI concept at ALOHA Station for 100 m depth.

Direct stabilization with surface mixing

This section examines the TAKUMI concept (Ouchi and Ohmura, 2004). It is represented here as the direct mixing of the lightest possible water, from the surface, with nutrient-rich deep seawater from a selected withdrawal depth. This is a simplification of the actual process implemented in Sagami Bay, since in a real system, mixing may be somewhat more complicated. The essence of the idea, however, is the same: to achieve the lowest possible dilution of the nutrient-rich water for a given neutral-buoyancy depth, or equivalently, to stabilize a mixture with a given S at the shallowest possible depth. In Sagami Bay, the nutrient-rich deep water from about 200 m had a temperature of about 10°C and nitrate concentration $[N]$ of 20 μM . Water with similar temperature and nitrate (plus nitrite) content typically is found at a depth of about 400 m at Station ALOHA (Flament et al., 1996). Therefore, a withdrawal depth of 400 m is

chosen in this study with little loss of generality.

Using monthly average profiles of salinity and temperature from the first 133 cruises of the HOT program, and the algorithm of Fofonoff and Millard (1983) to calculate potential density, it is straightforward to determine how the idealized TAKUMI concept would fare at Station ALOHA. Figures 1 and 2 show how much surface water should be mixed to 400 m deep water to vertically stabilize it at a given depth (designated as ‘mixture injection depth’). A thick line shows the same result for the yearly average profile of salinity and temperature from the HOT data base, and the Sagami Bay experiment is indicated as a square.

It is immediately apparent that conditions selected at Sagami Bay were extraordinarily favorable; the low mixing ratio of two and the shallow neutral-buoyancy depth of the order of 20 m were the result of a steep and shallow (Summer) density stratification. Such conditions cannot be found in the open

waters of tropical oceans. Instead, stable, deep and moderate density stratifications prevail. As a result, large mixing ratios are necessary to vertically confine a mixture of nutrient-rich deep water and surface water even at depths of the order of 100 m.

The seasonal trend in Figures 1 and 2 confirms that the TAKUMI concept would work relatively better in Summer months, when lighter surface water has a greater ability to stabilize a given mixture at a shallower depth. This is further illustrated in Figure 3, where the time course of the mixing ratio ($S - 1$) for stabilization at 100 m depth is given. A wide range for ($S - 1$), from a little over 2 to more than 10, is required at that depth ; the yearly calculation coincides with that for November.

These results may appear rather sobering to ‘artificial upwelling’ enthusiasts. The TAKUMI concept, however, has an advantage: the relationship between stabilization depth and nutrient dilution is essentially independent from the mass flow rate of the withdrawn deep water, inasmuch as pumping hardware and pipes allow. Finally, one may understand why the basic idea behind TAKUMI did not emerge in connection with OTEC. Since mixed OTEC effluents would correspond to low dilutions of the deep cold water (i.e. S of 2.5 to 3), a controlled discharge would have seemed attractive, but it is clear from Figures 1 and 2 that neutral-buoyancy depths would then be excessive³. Menesguen et al. (1989) further studied the feasibility of boosting primary productivity with OTEC effluent *plumes* (released at shallower depths) but their conclusions were not encouraging.

Negatively buoyant plumes

While the notion of directly mixing surface water and nutrient-rich deep water may not easily be implemented in tropical open-ocean conditions, it should nevertheless represent a best-case scenario regarding the ability to vertically stabilize deep nutrients into the upper water column. The classical approach to ‘artificial upwelling’ has been to consider the release of nutrient-rich deep water as a negatively buoyant plume in the upper waters.

A typical integral model of a negatively buoyant plume was implemented for this study, with ambient water-column characteristics corresponding to the yearly average of the first 133 HOT cruises, with little loss of generality. Transverse plume characteristics are assumed to be known, e.g. as Gaussian profiles; equivalent single-value ‘top-hat’ formulations are possible, and this choice was adopted here. A constant horizontal current U_a is allowed; in this case, the plume trajectory is not a vertical line, but must be determined. The x -axis is aligned with U_a and the vertical z -axis points downward. Nine variables are considered: mass flux ρQ , horizontal momentum flux M_x , vertical momentum flux M_z , horizontal centerline coordinate X , vertical centerline coordinate Z , and the fluxes (generically noted T) of four tracers: heat, salt, nitrate⁴ and chlorophyll-a⁴ (the last two are not relevant to plume stabilization, but will be considered later). The following set of ordinary differential equations was solved, with the right-hand-side of the first equation corresponding to the entrainment formalism of Hoult et al. (1969):

³As a matter of fact, OTEC mixed effluents would be harder to stabilize than inferred from Figures 1 and 2, since OTEC deep cold seawater typically is drawn from 1000 m depth; at best, and at the cost of substantial complications, the ‘direct mixing’ curve in Figures 1 and 2 could represent a mixture of surface seawater with the separate effluent from the OTEC condenser.

⁴This species is considered to be a tracer in near-field plume calculations because the time scale for plume settling is much smaller than the time scale for Gross Primary Production.

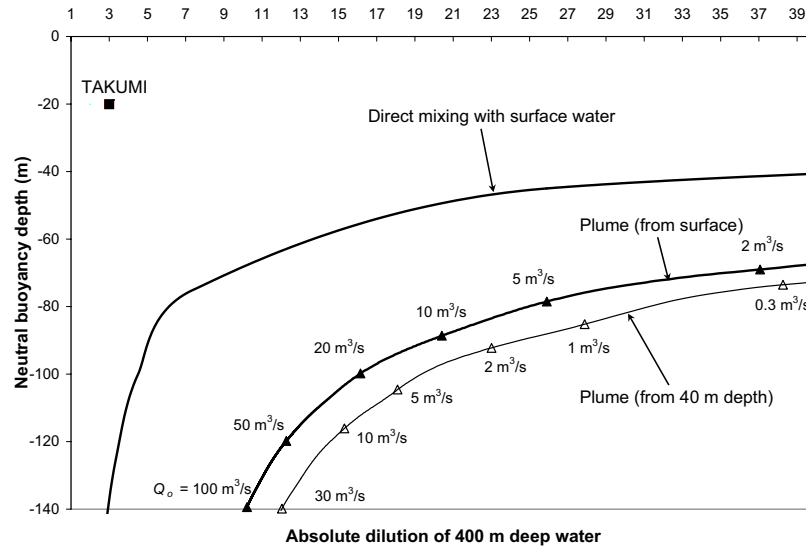


FIGURE 4
Absolute dilution as a function of settling depth for plumes with no crossflow at Station ALOHA.

$$\left\{ \begin{array}{l} \frac{d(\rho Q)}{ds} = 2\pi\rho_a b \{ \alpha | (u - U_o \cos\phi) | + \beta | U_o \sin\phi | \} \\ \frac{dM_x}{ds} = \frac{d(\rho Q)}{ds} U_o \\ \frac{dM_z}{ds} = \pi g b^2 (\rho - \rho_a) \\ \frac{dX}{ds} = \cos\phi \\ \frac{dZ}{ds} = \sin\phi \\ \frac{dT}{ds} = \frac{d(\rho Q)}{ds} T_o \end{array} \right. \quad (1)$$

ϕ is the angle of the plume trajectory from horizontal equal to $\tan^{-1}(M_z/M_x)$, g the acceleration of gravity, s the plume centerline curvilinear coordinate, u the plume centerline velocity equal to $M_z / (\rho Q \sin\phi)$, and b the plume radius equal to $\sqrt{Q/(\pi u)}$. The first term

in the right-hand-side of the equation for $d(\rho Q)/ds$ represents entrainment of ambient water into the plume from the relative velocity along the plume centerline. For buoyant plumes, much work has been expended to determine the first entrainment coefficient α ; Fisher et al. (1979) determined that a constant value of 0.12 yields satisfactory results⁵. The second term in the right-hand-side of the equation for $d(\rho Q)/ds$ represents entrainment of ambient water into the plume from the transverse component of the current. The second entrainment coefficient β was selected as 0.53 following Hewett et al. (1971).

Equations (1) were integrated from initial conditions with a 4th order Runge-Kutta method, using 2000 steps from $s = 0$ to $s = 200$ m. Initial plume characteristics (e.g. tracer concentrations, density) correspond to those of the released deep water. No initial horizontal

⁵ These workers proposed $\alpha = 0.083$ for Gaussian plume profiles; with the equivalent top-hat formulation adopted here, this value must be multiplied by $\sqrt{2}$.

momentum flux and a small initial vertical momentum flux (corresponding to a downward velocity of 0.05 m/s) were selected. As earlier, water withdrawn from a depth of 400 m was selected to define initial plume characteristics at release.

Cases without crossflow

Cases with $U_a = 0$ were first considered. This situation may better apply to the futuristic concept of 'drifting sea ranch' (Takahashi et al., 1993). As expected, larger surface releases of deep water settle at greater depths h_T but undergo less dilution. Figure 4 includes a plot of $S = Q/Q_o$ at neutral buoyancy versus depth h_T for plumes with Q_o up to 100 m³/s. It can be seen that the TAKUMI concept is always more effective, as expected.

Also shown are calculations when plumes are released at a depth of 40 m. In this case, a greater penetration of the water column is achieved, but with less dilution, as confirmed in Liu et al. (2003). Whether sub-surface releases may be advantageous depends on biological responses in the presence of enhanced levels of nutrients and reduced light availability. This type of tradeoff may better be understood from the discussion of Gross Primary Production in the next Section.

Of interest is the time it takes for the released deep water to reach the region of plume neutral buoyancy at depth h_T . This plume settling time τ simply is $\int_0^{h_T} \frac{dz}{u(z)}$. For plumes with Q_o from 0.1 to 10 m³/s, τ ranges from 5 to less than 8 minutes; larger plumes would sink even faster. Hence, biological activity should be negligible in this near-field phase.

Without performing plumes calculations, it is possible to estimate both h_T and $S(h_T)$.

For environments where the buoyancy frequency $N = [(g/\rho)d\rho/dz]^{1/2}$ is nearly constant, Morton et al. (1956) proposed the formula:

$$h_T \approx 3.79 B_o^{1/4} N^{-3/4} \quad (2)$$

where B_o is the initial buoyancy flux equal to $Q_o g(\rho_o - \rho_s)/\rho_s$; ρ_s and ρ_o are the potential densities for surface and nutrient-rich deep seawater, respectively. For general cases where N varies with depth, a representative value of the buoyancy frequency in the surface⁶ layer of thickness h_T could be used in the formula. Both the average of N and the square root of the average of $(g/\rho)d\rho/dz$ were considered. Because of the averaging process, Equation (2) is now implicit with respect to h_T . With Q_o equal to 0.1, 1.0 or 10 m³/s, estimates of h_T were within 6.6 % of the values obtained by solving Equations (1). Wright (1977) suggested that when $N = 0$ (no stratification), $Q \approx 0.20 B_o^{1/3} z^{5/3}$. Nihous (2003) found that an integral plume model with $\alpha = 0.15$ yielded similar results. Substituting h_T for z , and adjusting the coefficient from 0.20 to 0.16 since $\alpha = 0.12$ was adopted here, $S(h_T)$ may be approximated by the following relationship:

$$S(h_T) \approx 0.16 B_o^{1/3} h_T^{5/3} Q_o^{-1} \quad (3)$$

With Q_o equal to 0.1, 1.0 or 10 m³/s, estimates for $S(h_T)$ from Equation (3) were within 9.8 % of the values obtained by solving Equations (1).

Cases with crossflow

Cases with $U_a = 0.1$ m/s were then examined to evaluate the effect of modest horizontal

⁶'surface' as well as h_T are referred to the plume origin; this should be taken into account for plumes originating below the ocean surface.

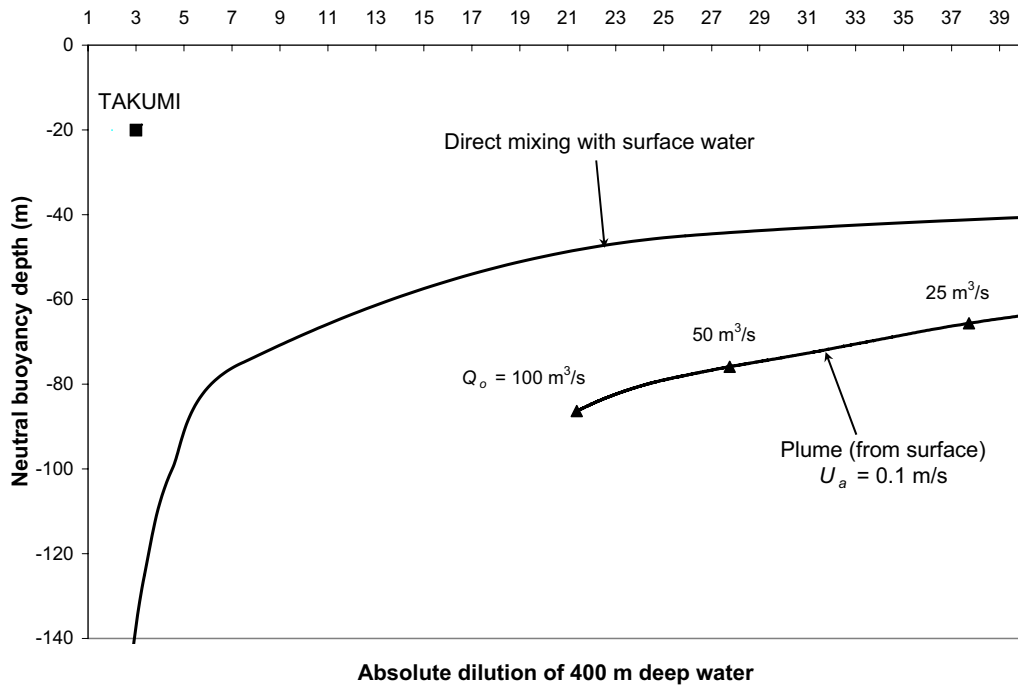


FIGURE 5
Absolute dilution as a function of settling depth for plumes in a 0.1 m/s crossflow at Station ALOHA.

cross-currents on plume characteristics, e.g. when the plume release is a fixed point. Equations (1) allow the input of a stratified current field so that the example under consideration is a simplification. Typical plume trajectories undergo oscillations after reaching neutral buoyancy; the wavelength λ of these oscillations is the product of the current velocity U_a times the local buoyancy period $2\pi/N(h_T)$. h_T is defined here as the average between the first (overall) maximum and the next (relative) minimum of Z . As expected, plumes of given initial characteristics stabilize at shallower depths with increased dilution in the presence of currents. Figure 5 is the equivalent of Figure 4 with the 0.1 m/s horizontal cross-flow. While the shape of the curve $S(h_T)$ hardly changes, each point

corresponds to Q_o about one order of magnitude higher when $U_a = 0.1$ m/s.

As before, it is possible to estimate h_T with a simple approximate formula. Hewett et al. (1971) proposed the following equation for h_T when N is constant:

$$h_T \approx 1.7 \{B_o / (U_a N^2)\}^{1/3} \quad (4)$$

With Q_o equal to 0.1, 1.0 or 10 m³/s, estimates of h_T using the same implicit procedure applied to Equation (2) were within 8.8 % of the values obtained by solving Equations (1). Trying, however, to use the curve fit of Huang et al. (1998) for the volume flow rate of plumes in cross currents but without stratification greatly underestimated dilution; this was attributed to the substantial

additional mixing affecting a plume as it nears neutral-buoyancy depth and begins oscillating in advected stratified waters.

Summary

Values of h_T and $S(h_T)$ of about 60 m and 10, respectively, are often considered 'ideal' for AU systems (e.g. Liu et al., 2003). None of the cases shown in Figures 4 and 5 are likely to meet this target, even though a direct mixing process may seem close enough. Liu et al. (2003) argued that combining a deep release (40 m) with a 75% reduction of B_o would work, at least with $U_a = 0$ and Q_o of the order of $1 \text{ m}^3/\text{s}$. Yet, it is shown in Appendix A that the reduction of B_o by 'raising the temperature of the effluent' as suggested, would be very costly. Desirable targets such as $h_T \approx 60 \text{ m}$ and $S(h_T) \approx 10$ may actually be too strict, and an objective evaluation of 'plume performance', i.e. any tradeoff between near-field dilution and neutral-buoyancy depth, should involve the ability of phytoplankton to process the upwelled nutrients.

GROSS PRIMARY PRODUCTION (GPP) IN OLIGOTROPHIC WATERS

The objective of making nutrients found at high concentrations in deep waters available at or near the ocean surface is to enhance photosynthesis. GPP affects the lowest fundamental level of the oceanic food web, and boosting it eventually could increase stocks at higher trophic levels. In spite of the complex phenomena involved, simple representations of GPP for modeling purposes have been available. Recent examples which provide a basis for the

approach adopted here may be found in Kawamiya et al. (1995), Kishi et al. (2001) and Yanagi et al. (2001). More detailed formalisms, based for example on the concept of quantum yield, have been developed and could be used instead (Wozniak et al., 2002; for the subtropical North Pacific, cf. Ondrusek et al., 2001).

In oligotrophic oceanic regions, however, nutrients are only present at nanomolar levels, and the kinetics of nutrient uptake appears to be adapted to near-depletion conditions. In fact, a great deal of phytoplankton growth recycles nitrogen from waste (ammonium, urea). For this reason, and assuming that nitrogen availability is limiting, we will consider the nitrogen utilization formalism of Harrison et al. (1996).

The rate GPP at which phytoplankton concentration, expressed as $[Chl a]$, increases via photosynthesis is written:

$$GPP = [V_A \frac{[A]}{K_A + [A]} + V_N \frac{[N]}{K_N + [N]} (1 - \frac{I_m [A]}{K_i + [A]})] A_\theta A_{light} [Chl a] \quad (5)$$

$[A]$ and $[N]$ are the concentrations of ammonium and of nitrate (plus nitrite), respectively. K_A and K_N are the respective half-saturation constants. V_A and V_N are reference rates with respect to ammonium and nitrate uptake, respectively. The factor $(1 - \frac{I_m [A]}{K_i + [A]})$ represents ammonium inhibition of nitrate uptake, and depends on two constants I_m and K_i . A_θ represents the potential influence of temperature θ , since colder water may inhibit growth. In Kishi et al. (2001), this term is represented as $\exp\{k(\theta - \theta_{ref})\}$, with $\theta_{ref} = 0^\circ\text{C}$; here, θ_{ref} is defined as the sea surface temperature. It has been recognized, however, that temperature has a greater influence in selecting species than in controlling biomass (Vaulot, 2001). Light limitation has been investigated extensively,

TABLE 1A
Selected parameters in Equation (5) for HOT data10^a.

I_s/I_{opt}	k (°C ⁻¹)	κ (m ⁻¹)	K_N (nM)	K_A (nM)	K_i (nM)	I_m	V_N (day ⁻¹)	V_A (day ⁻¹)	[A] (nM)	C:N (molar)
1.35	0.063	0.035	30	10	60	0.60	0.4	2.0	40	106:16
1.35	0	0.035	30	10	50	0.67	0.4	2.0	40	106:16

^aInput ([N], θ , [Chl a] as a function of depth) and targets (GPP as a function of depth and [PON] flux at 150 m) are averages through 133 HOT cruises.

TABLE 1B
Selected parameters in Equation (5) for the data of Allen et al. (1996)^a.

Station ^b	I_s/I_{opt}	K_N (nM)	K_A (nM)	K_i (nM)	I_m	V_N (day ⁻¹)	V_A (day ⁻¹)	[A] (nM)
2	1.8 ^c	30	10	100	0.5	2.1	2.1	40
	1.8 ^c	30	200	2000	0.5	2.1	2.1	851 ^d
6	1.35	30	10	50	0.6	1.0	1.9	40
	1.35	30	200	1000	0.6	1.0	1.9	1080 ^d
10	1.0	30	10	50	0.6	1.8	0.36	40
	1.35	30	10	50	0.6	1.1	2.0	1.5
	1.1	30	2000	2000	0.6	1.4	1.4	860 ^d

^aNo temperature effect. Input (Relative light level, [N] and [Chl a] as a function of depth) and targets (GPP, Autotrophic nitrogen assimilation and NP integrated down to the 0.1% light level) are from Allen et al. (1996).

^bStation 10 is inside the cyclonic eddy.

^cValue given in Allen et al. (1996).

^d[A] data as a function of depth from Allen (1994); value listed is average down to 0.1% light level.

TABLE 1C
Selected parameters in Equation (5) for the data of Vaillancourt et al. (2003)^a.

Station ^b	κ (m ⁻¹)	I_s/I_{opt}	K_N (nM)	K_A (nM)	K_i (nM)	I_m	V_N (day ⁻¹)	V_A (day ⁻¹)	[A] (nM)
1	0.043 ^a	1.8	30	8	100	0.5	2.0	2.1	59 ^{ac}
2	0.066 ^a	1.9	30	10	100	0.5	2.1	1.0	27 ^{ac}
3	0.063 ^a	1.9	27	10	100	0.5	2.1	1.0	18 ^{ac}

^aNo temperature effect. Input (κ ; [N] and [Chl a] as a function of depth) from Vaillancourt et al. (2003); input ([A] as a function of depth) from Bidigare (2005); target (GPP integrated down to 150 m) from Bidigare et al. (2003).

^bStations 2 and 3 are inside the cyclonic eddy.

^cValue listed is average down to 150 m.

i.e. by Platt et al. (1980). Many simple analytical functions may adequately fit the relationship between light intensity and phytoplankton behavior. The expression proposed by Kishi et al. (2001) was adopted:

$$A_{light} = \frac{I_s \exp(-\kappa z)}{I_{opt}} \exp\left\{1 - \frac{I_s \exp(-\kappa z)}{I_{opt}}\right\} \quad (6)$$

where κ is the light extinction coefficient, and I_s and I_{opt} are the surface and optimum light intensities, respectively. Because of photoinhibition near the ocean surface, I_{opt} is less than I_s . A value κ of 0.035 m^{-1} corresponds to a 0.1% level (relative to surface irradiance) at a depth just above 200 m.

Of particular interest is the *f-ratio*, which expresses the relative amount of New Production (NP), over GPP. New Production is given by:

$$NP = [V_N \frac{[N]}{K_N + [N]} (1 - \frac{I_m[A]}{K_i + [A]})] A_0 A_{light} [Chl a] \quad (7)$$

When *GPP* and *NP* must be expressed in mass units of carbon (e.g. $\text{mg C/m}^3\text{-day}$), a phytoplankton mass ratio of carbon to chlorophyll-*a* equal to 50 is used. Oligotrophic waters are characterized by low values of the *f-ratio*. Also typical are nanomolar values of the half-saturation constants in Equation (5).

A definition of the parameters in Equation (5), with or without temperature effect, was attempted by fitting measured profiles of Gross Primary Production averaged over all HOT cruises to date. The corresponding HOT data for θ , $[N]$ and $[Chl a]$ also was used as an input. Initial guesses for the nutrient uptake coefficients relied mostly on the oceanic values proposed in Harrison et al. (1996). Since ammonium concentrations were reported to be “below the (50 nM) detection limit of standard nutrient analyses” (Fujieki et al., 2004), a constant value $[A]$ ($< 50 \text{ nM}$) was assumed. An

additional constraint was the average flux of Particulate Organic Nitrogen (*PON*) at 150 m, equal to $4.2 \text{ mg-N/m}^2\text{-day}$ from the overall HOT time series. This is a measure of integrated New Production in the upper 150 m. With an organic C:N molar ratio taken to be 106:16, the *PON* flux at 150 m corresponds to $23.85 \text{ mg-C/m}^2\text{-day}$. Selected parameters are listed in Table 1a. Choices for V_N and V_A are consistent with the fact that ammonium uptake always was found to exceed nitrate uptake in Harrison et al. (1996). A more detailed discussion of these photosynthetic rates can be found in Appendix B. Figure 6 and Table 2a show excellent agreement between the data and calculations from Equation (5). Since the temperature effect appears minimal, it will be ignored henceforth with little loss of generality.

Mesoscale cold-core cyclonic eddies are periodically generated in the lee of the Big Island of Hawaii. A mechanism for their formation is shown schematically in Flament et al. (1996). While these eddies are sustained, nutrient upwelling occurs. Primary productivity characteristics associated with this phenomenon were investigated (Allen et al., 1996; Vaillancourt et al., 2003; Bidigare et al., 2003). Tables 1b and 1c show a selection of parameters in Equation (5) that would produce a good match with the data of Allen et al. (1996) and Vaillancourt et al. (2003), respectively, as shown in Tables 2b and 2c. Ammonium concentrations measurements from Allen (1994) probably were contaminated, though choosing much higher values of K_A and K_i would mask this. Data from Vaillancourt et al. (2003) for the light extinction coefficient κ clearly show self-shading within the eddy (Stations 2 and 3). A consistent result is a much higher *f-ratio* inside the eddy, of the order of 0.8, or four

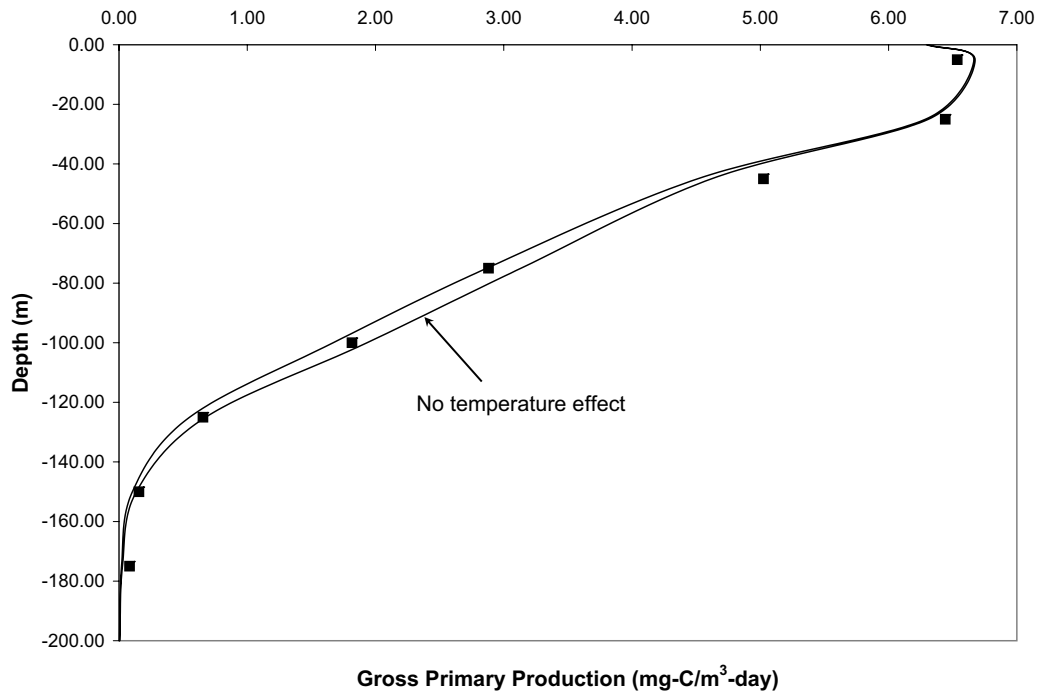


FIGURE 6
Calculated GPP profiles (lines) and average HOT data (“Light 12”) at Standard Depths (squares).

times values just outside⁷. An interesting fact in the parameter selection process is the apparent need for relatively higher values of V_N (which sometimes exceed V_A). This could merely show that Equation (5) is an oversimplification of real processes; it might also indicate a community shift in the phytoplankton population (a relative dominance of large photosynthetic eukaryotes inside the eddy is reported in Vaillancourt et al., 2003).

For a practical near-field evaluation of AU concepts, the most consistent and most significant point from basic models of GPP in oligotrophic waters may be extremely low values of the half saturation coefficient K_N , of the order of 30 nM.

NEAR-FIELD BIOLOGICAL INDICES OF PERFORMANCE

We are now in a position to define several near-field indices of performance for the two AU concepts discussed earlier (direct mixing with surface water, and negatively buoyant plumes). The basis for evaluation will be the potential of a concept to boost New Production. Assuming that $[A]$ is constant and without temperature effect, Equation (7) suggests that the following function is representative of the potential for New Production:

$$F = \frac{[N]}{K_N + [N]} [Chl a] A_{light}$$

⁷ The integrated f -ratio for the oligotrophic open-ocean HOT data is only about 0.1.

TABLE 2A
Results from Equation (5) and average HOT data.

	GPP profile (mg-C/m ³ -day)	GPP integrated to 200 m (mg-C/m ² -day)	NP integrated to 150 m (mg-C/ m ² -day) ^a
Data		498	23.85
“ θ effect”	cf. Fig. 6	475	23.70
“No θ effect”	cf. Fig. 6	496	23.80

^aN molar ratio of 106:16 assumed to convert from mg-N/m²-day.

TABLE 2B
Results from Equation (5)^a and data of Allen et al. (1996).

	GPP integrated to 0.1% light level (mg-C/m ² -day)	Average f -ratio ^{bc}
Station 2 data	399 (132 m)	0.20 (C:N = 7.82)
“[A] = 40 nM”	393	0.196
“[A] data” ^d	392	0.195
Station 6 data	523 (135 m)	0.19 (C:N = 5.34)
“[A] = 40 nM”	533	0.199
“[A] data” ^d	538	0.190
Station 10 data	662 (181 m)	0.81 (C:N = 6.02)
“[A] = 1.5 nM”	673	0.789
“[A] = 40 nM”	673	0.803
“[A] data” ^d	670	0.795

^aExp(- κz) replaced by Relative light level data in Equation (5)

^bdefined as ratio of NP integrated to 0.1% light level (in mg-N/m²-day) over autotrophic nitrogen assimilation integrated to 0.1% light level

^cCarbon to nitrogen conversions from average C:N mass ratio, provided as ratio of GPP integrated to 0.1% light level over autotrophic nitrogen assimilation integrated to 0.1% light level

^dFrom Allen (1994)

TABLE 2C
Results from Equation (5) and data of Vaillancourt et al. (2003).

	GPP integrated down to 150 m (mg-C/m ² -day)	Average f -ratio ^a
Station 1 data	670 ^b	N/A
Equation (5)	668	0.199
Station 2 data	870 ^c	N/A
Equation (5)	403	0.805
Station 3 data	870 ^c	N/A
Equation (5)	870	0.675

^aDefined as ratio of NP integrated down to 150 m (in mg-C/m²-day) over GPP integrated down to 150 m.

^bAverage of three Stations outside cyclonic eddy, from Bidigare et al. (2003).

^cAverage of three Stations inside cyclonic eddy, from Bidigare et al. (2003).

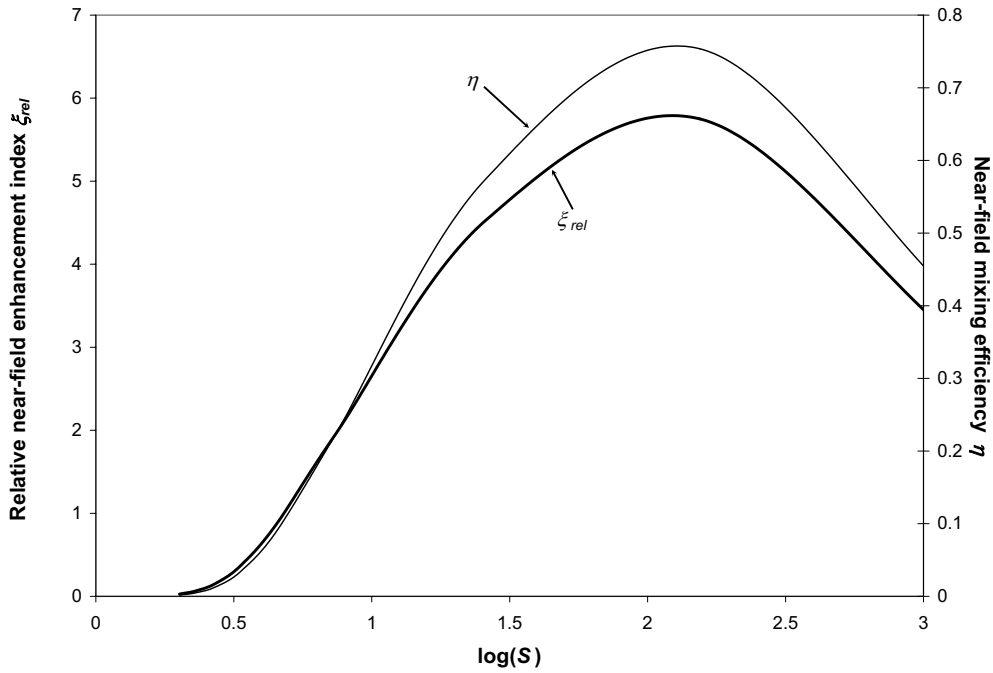


FIGURE 7 Near-field mixing efficiency and relative near-field enhancement index for the direct mixing concept (yearly HOT data and 400 m deep nutrient-rich water).

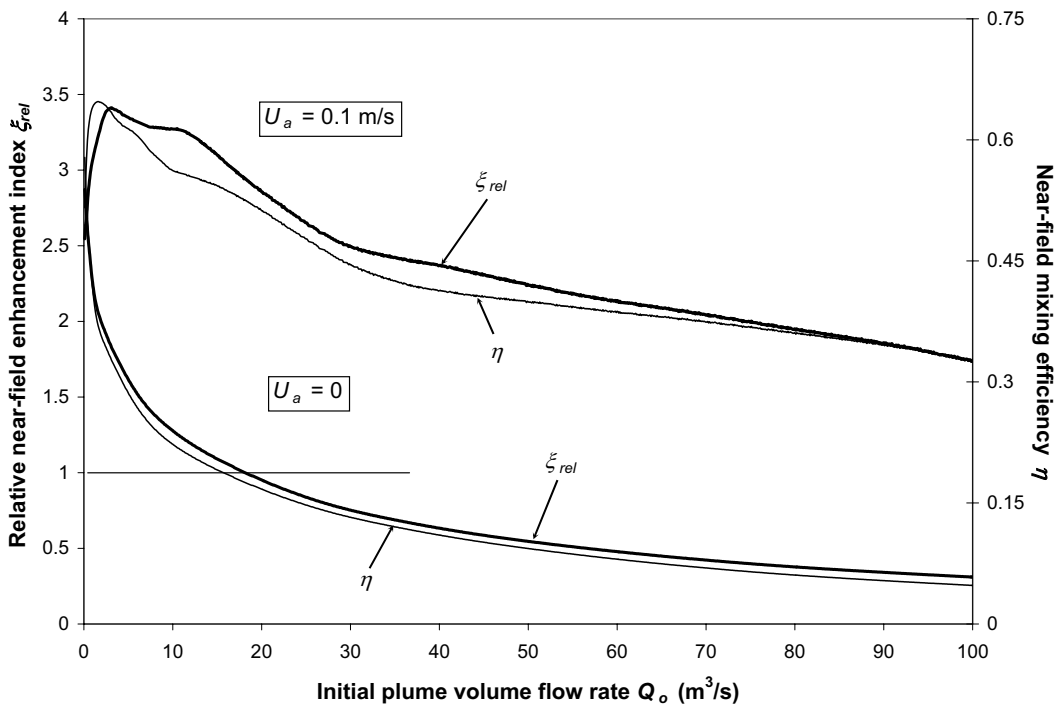


FIGURE 8 Near-field mixing efficiency and relative near-field enhancement index for sinking plumes (yearly HOT data and 400 m deep nutrient-rich water).

Results for plumes will be presented as functions of the volume flow rate of deep nutrient-rich water Q_o . This would be the amount of water to be handled in AU systems generating negatively buoyant plumes. For the direct mixing concept, results are independent of Q_o as long as a required mixture of deep and surface waters is achieved for a selected stabilization depth. While such independence appears to be a considerable advantage, the direct mixing concept relies on handling *both* deep and surface seawater flow rates. Overall seawater flow rates are well reflected in the dilution ratio S . As S increases for shallower stabilization, the concept would in effect become impractical unless Q_o remains quite small. Direct-mixing results then will be shown as functions of S and their practicality discussed in the context of ‘small enough’ S .

Mixing efficiency

For deep nutrient-rich seawater, $[Chl\ a]$ is zero so that ‘upwelled’ water by itself theoretically cannot sustain primary production until it gets mixed ($F_o = 0$). This will occur through plume dynamics, turbulent diffusion, wave action etc. Not surprisingly, Kajikawa (1997) reported that in the Toyama Bay AU experiments, mixing upwelled water with surface water reduced the “lag period of phytoplankton growth”. Since too much dilution would not promote new growth either, with $[N]$ for the mixture becoming very small, there mathematically must exist an optimal mixing ratio ($S_{opt} - 1$) that maximizes F/A_{light} to a value $(F/A_{light})_{max}$. Expressing the condition $d(F/A_{light})/dS_{opt} = 0$ with mixture values $[N] = \{(S_{opt} - 1) [N]_s + [N]_o\} / S_{opt}$ and $[Chl\ a] = (S_{opt} - 1) [Chl\ a]_s / S_{opt}$, elementary but cumbersome algebra yields:

$$S_{opt} = 1 + \frac{[N]_s(K_N + [N]_o) + ([M]_o - [N]_s)\sqrt{K_N(K_N + [N]_o)}}{K_N[N]_o - [N]_s^2 - 2K_N[M]_s}$$

With $[N]_o \gg [N]_s$ and $[N]_o \gg K_N$, it can easily be shown that $S_{opt} \approx 1 + \sqrt{[N]_s/K_N}$. The overall HOT average for $[N]_o$ at 400 m depth is 18.227 $\mu\text{mol/kg}$. With $K_N = 30$ nM, we find that $S_{opt} = 25.82$. In other words, a fairly large dilution may not be so detrimental in triggering New Production since K_N is small (oligotrophic waters).

A measure of the mixing efficiency of an AU system to provide near-field conditions favorable to New Production may be defined as $\eta = F(h_T)/(F/A_{light})_{max}$. In this expression, the denominator implicitly has been multiplied by the maximum value of A_{light} , i.e. one.

Figures 7 and 8 show η either as a function of $\log(S)$ or as a function of Q_o for the direct-mixing and plume concepts, respectively. It is apparent in Figure 8 that a modest horizontal current has a profound effect on plume mixing characteristics: while the additional plume dilution produced by cross flows may be detrimental per se, this relative ‘loss’ is more than offset by the photosynthetic advantage of much shallower neutral-buoyancy depths. When considering Figure 7, the practical expectation that Q_o should not be too small imposes in turn a practical limit on S : for example, if $Q_o = 10$ m^3/s were envisioned, a value $S = 10$ (i.e. $\log(S) = 1$) would imply the overall handling of 100 m^3/s . Thus, values corresponding to $S < 10$ might very well represent a practical range of interest for the direct-mixing concept; in this interval, η is not very high.

RELATIVE NEW PRODUCTION ENHANCEMENT POTENTIAL

Another way to gauge the near-field effectiveness of AU strategies is to quantify relative New Production enhancement by comparing the flux of F at neutral buoyancy

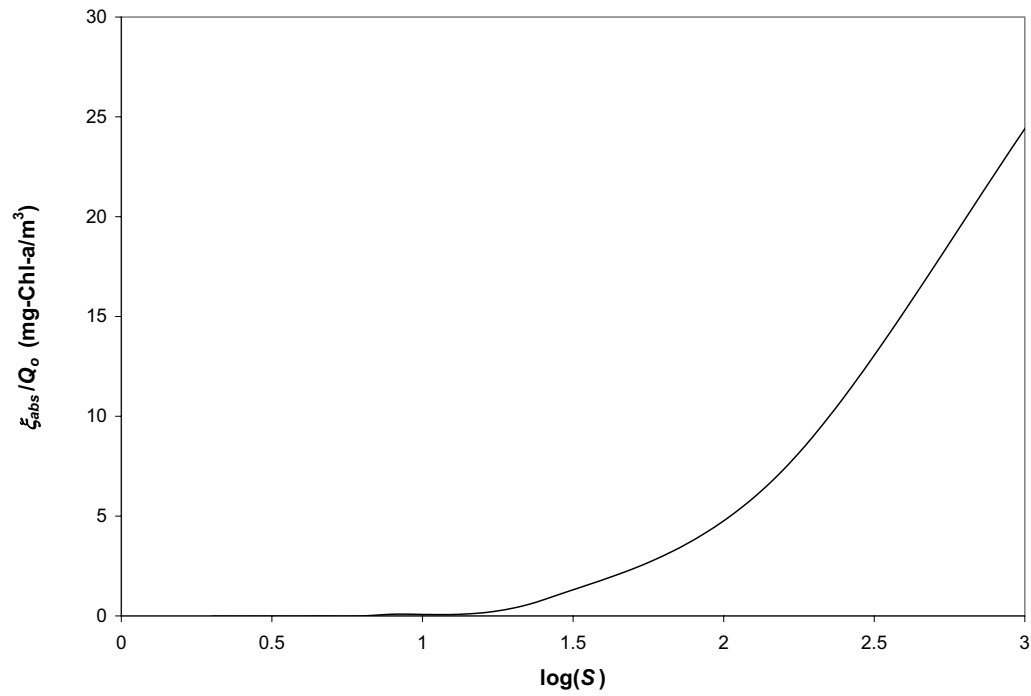


FIGURE 9
Absolute near-field enhancement index per unit flow rate of deep nutrient-rich water for the direct mixing concept.

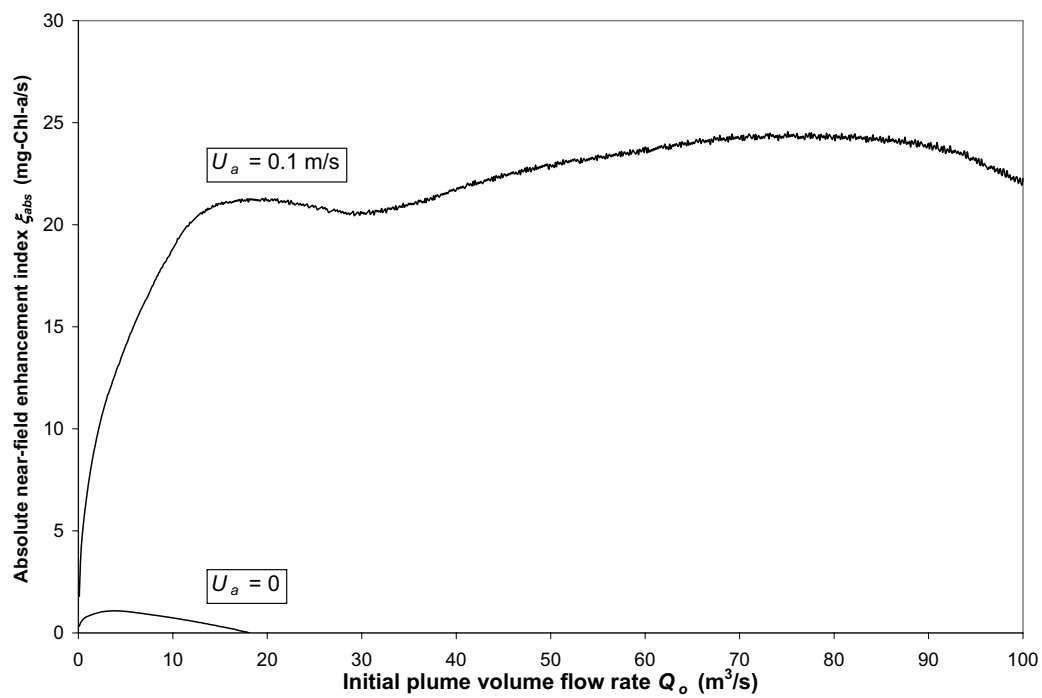


FIGURE 10
Absolute near-field enhancement index for sinking plumes: yearly HOT data and 400 m deep nutrient-rich water.

with the integrated F -flux contributions of the water masses involved in the AU process. Recalling that $F_o = 0$, a relative near-field enhancement index ξ_{rel} for negatively buoyant plumes may therefore be written:

$$\xi_{rel} = \frac{Q(h_T)F(h_T)}{\int_{Q_s}^{Q(h_T)} F_a dQ}$$

For the direct-mixing concept, an equivalent definition is $\xi_{rel} = \frac{S(h_T)F(h_T)}{[S(h_T)-1]F_s}$.

ξ_{rel} is displayed on Figures 7 and 8 for both types of AU systems. It is clear that aside from different scales, the two performance indices η and ξ_{rel} are very similar. It should be noted that if $\xi_{rel} < 1$, the overall AU process would result in a near-field reduction of New Production potential, i.e. the opposite of the desired objective.

Absolute New Production enhancement potential

The most important measure of success for any given AU strategy would be its ability to enhance oceanic productivity in absolute terms. If the idea were ever implemented, its ultimate goal would be to boost output from the entire food chain. A near-field ‘first step’ for this to happen would depend on some absolute New Production enhancement potential. Accordingly, an absolute near-field enhancement index ξ_{abs} for negatively buoyant plumes may be written as $\xi_{abs} = \frac{Q(h_T)F(h_T) - \int_{Q_s}^{Q(h_T)} F_a dQ}{[S(h_T) - 1]F_s}$. Although ξ_{abs} has dimensions (mg-Chl-a/s), one should refrain from inferring actual productivity until a far-field, biologically coupled model is developed⁸. For the direct-mixing concept, we must define $(\xi_{abs}/Q_o) = \frac{S(h_T)F(h_T) - [S(h_T) - 1]F_s}{Q_o}$ instead, in units of mg-Chl-a/m³.

Figures 9 and 10 show ξ_{abs}/Q_o and ξ_{abs} for the direct-mixing and plume concepts, respectively. In Figure 10, the difference between cases with $U_a = 0$ or $U_a = 0.1$ m/s is very pronounced. The beneficial effect of a small current is crucial in sustaining absolute enhancement as Q_o increases. Also, there is an apparent limit for ξ_{abs} as Q_o approaches values of the order of 10 to 20 m³/s. This would suggest that very high flow rates Q_o may never be warranted. Also, Figure 9 does not show the direct-mixing concept in a favorable light for open-ocean oligotrophic conditions; if $Q_o = 10$ m³/s were targeted, for example, a value $\xi_{abs} = 8.6$ mg-Chl-a/s would correspond to $S = 25.9$ and a very large combined flow of about 260 m³/s: this would not match the value $\xi_{abs} = 18.8$ mg-Chl-a/s obtained from Figure 10 and $U_a = 0.1$ m/s.

CONCLUSIONS

This study has succinctly reviewed the near-field behavior of artificially upwelled deep nutrient-rich water in open-ocean oligotrophic conditions. To this end, ample use of the Hawaii Ocean Time-series data base was made to characterize background conditions. Two basic concepts were considered: negatively buoyant plumes released at or near the surface, or the product of directly mixing deep and surface waters in a prescribed ratio.

It was verified that direct mixing is more effective in principle in vertically stabilizing a given water mixture. Because of a deep quasi-permanent stratification of the tropical open-ocean water column, however, direct mixing requires considerably greater dilution than was

⁸Gross Primary Production and far-field transport mechanisms (e.g. turbulent diffusion) essentially share similar time scales; GPP is only a source in the equations describing the evolution of phytoplankton biomass, and phytoplankton only represents one trophic level.

necessary during a recent summertime test in Sagami Bay, Japan. This may place substantial engineering limitations on this concept if applied to tropical open oceans, unless very small deep water flow rates are envisioned.

A brief consideration of Gross Primary Production in oligotrophic waters confirmed that standing phytoplankton populations are well adapted to nanomolar nitrate concentrations. Hence, a modest dilution of artificially upwelled nutrients may not be detrimental in boosting primary productivity.

When considering the near-field biological enhancement potential of negatively buoyant plumes, the beneficial role of a small horizontal cross flow of the order of 10 cm/s was suggested. This would result from a positive tradeoff between a shallower neutral- buoyancy depth within the photic layer and a greater dilution. It also appeared that the absolute near-field enhancement potential might level off for deep water flow rates exceeding 10 to 20 m³/s.

In all cases, a full model integrating far-field transport phenomena and the evolution of the lowest trophic levels would be warranted. This would help in assessing any risk that a particular AU system might have serious adverse effects as well as potential benefits. While any future AU at-sea test may be enlightening, further studies of the response of marine ecosystems to natural nutrient enhancement (e.g. in intermittent cold core eddies) would be invaluable as well.

APPENDIX A

Temperature control of initial plume buoyancy

The ‘upwelled’ seawater is warmed until a targeted reduction of its excess density (and

hence B_o) is achieved. Let us assume that the warming of a flow rate Q_o at temperature θ_o is achieved in a countercurrent water-water heat exchanger with a flow rate Q_s of surface water at temperature θ_s , as sketched in Figure A-1. The overall heat transfer coefficient H can be expected to be of the order of 1000 W/m²-K (e.g. Kreith and Bohn, 1973, p. 509). Within the range under consideration, the specific heat per unit volume ρc_p is practically a constant and equal to 4000000 J/m³-K.

The thermal power q gained by the ‘upwelled’ water is equal to the thermal power lost by the ambient seawater circulating in the heat exchanger. It follows that:

$$q = Q_s \rho c_p (\theta_s - \theta_{s,out}) = Q_o \rho c_p (\theta_{o,out} - \theta_o) \quad (A-1)$$

The heat exchanger area A can be determined from the classic formula (Kreith and Bohn, 1983):

$$A = \frac{q}{H \Delta\theta_{LMTD}} \quad (A-2)$$

where the Logarithmic Mean Temperature Difference $\Delta\theta_{LMTD}$ is equal to:

$$\Delta\theta_{LMTD} = \frac{\Delta\theta_A - \Delta\theta_B}{\text{Log}\left(\frac{\Delta\theta_A}{\Delta\theta_B}\right)}$$

the auxiliary temperature differences $\Delta\theta_A$ and $\Delta\theta_B$ are defined in Figure A-1; in the special case $Q_s = Q_o$, $\Delta\theta_{LMTD} = \Delta\theta_A = \Delta\theta_B$.

The heat exchanger should be designed to achieve a fixed value of $\Delta\theta_A$, in order to control the density of the ‘upwelled’ water as it exits; for given seawater flow rates, Equation (A-1) yields $\theta_{s,out}$. $\Delta\theta_B$ is then known, and after computing $\Delta\theta_{LMTD}$, one obtains A from Equation (A-2).

Let us consider the 75% reduction of excess density suggested by Liu et al. (2003) for Q_o

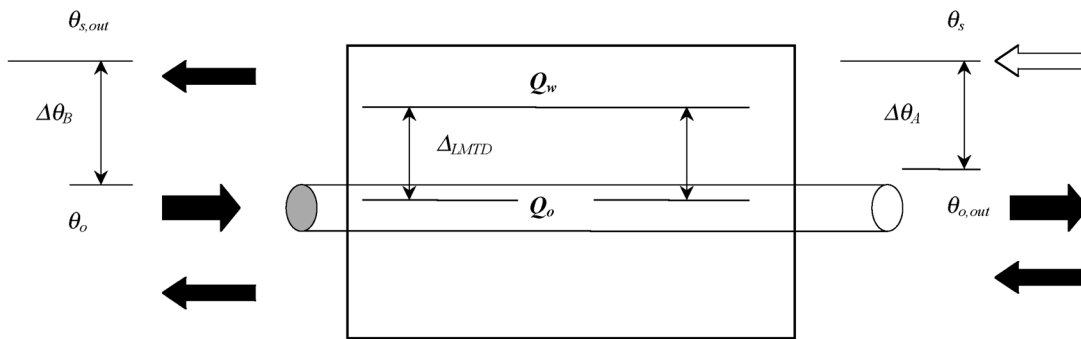


FIGURE A-1
Schematic diagram of a countercurrent heat exchanger.

of the order of $1 \text{ m}^3/\text{s}$. From the averaged HOT data for water upwelled from a depth of 400 m, $\rho_o - \rho_s = 1026.34 - 1023.42 = 2.92 \text{ kg/m}^3$. After warming, the upwelled water should have a potential density of 1024.15 kg/m^3 ; with a salinity of 34.14 ppt, this corresponds to a temperature of 18.5°C ⁹. It follows that $\Delta\theta_A = 24.91 - 18.5 = 6.41 \text{ K}$.

With $Q_s = Q_o = 1 \text{ m}^3/\text{s}$, a heat exchanger corresponding to $A = 5554 \text{ m}^2$ would be required. If $Q_s = 2Q_o = 2 \text{ m}^3/\text{s}$, A would be reduced to 4307 m^2 .

These basic considerations show that large heat exchangers and large flow rates of ‘auxiliary’ surface water may be required even with small prototypical flow rates. The location of the intake and discharge points for the ‘auxiliary’ water would be critical as well to avoid any interference with the plume of nutrient-rich deep water.

APPENDIX B

Notes on the maximum daily photosynthetic rate V

Equation (6) contains the term I_s corresponding to daily surface irradiance. This concerns Photosynthetically Available Radiation (PAR) with wavelengths in the range 400 to 700 nm. Assuming light intensity to be a cosine function centered around Noon, and 12 hour wide (from 6:00 am to 6:00 pm), the daily average I_s is $2/\pi$ the maximum intensity I_{max} . PAR deck irradiance measured through HOT cruises 1-133 has a mean value of $43.35 \text{ E/m}^2\text{-day}$; this would correspond to $I_{max} = 1576.25 \text{ } \mu\text{E/m}^2\text{-s}$.

Harrison et al. (1996) report hourly maximum nitrogen uptake rates $\rho_m(N)$ and $\rho_m(A)$ from 3-hour midday incubation experiments under surface light. With the appropriate conversion factor between ρ_m and $[Chl a]$, we have the following relationship:

⁹Because deep water is about 1 ppt less saline, this temperature is colder than that of water with an *in situ* potential density of 1024.15 kg/m^3 by about 4°C .

$$V A_{light} [Chl a] = 3\rho_m \frac{\int_{Noon-1.5}^{Noon+6} \cos[\frac{\pi}{12}(t-noon)] \exp\{1 - \frac{I_{max}}{I_{opt}} \cos[\frac{\pi}{12}(t-noon)]\} dt}{\int_{Noon-1.5}^{Noon+1.5} \cos[\frac{\pi}{12}(t-noon)] \exp\{1 - \frac{I_{max}}{I_{opt}} \cos[\frac{\pi}{12}(t-noon)]\} dt} \quad (B-1)$$

t is the time in hour measured from Noon; A_{light} and $[Chl a]$ in the left-hand-side are surface values. With the ratio I_s/I_{opt} selected as 1.35 in Table 1a, $I_{max}/I_{opt} = 2.12$. Calculation of the integrals in Equation (B-1) is straightforward. With $[Chl a]$ in $\mu\text{g/l}$ and ρ_m in nM-N per hour, Equation (B-1) then reduces to $V = 0.0221 \rho_m/[Chl a]$. Using this expression, the open-ocean data of Harrison et al. (1996) has been ‘translated’ in terms of V , as shown in Table B-1. The selection $V_n = 0.4 \text{ day}^{-1}$ and $V_A = 2.0 \text{ day}^{-1}$ in Table 1a compares well with those inferred values.

Finally, Ondrusek et al. (2001) report near-surface values of the maximum rate of photosynthesis approximately between 5 and 10 mg-C per mg-Chl per hour, with Station ALOHA at the lower end of this range (their

Fig. 3 and Fig. 8a). With $A_{light} = 1$ in Equation (5), the maximum rate of photosynthesis is about 82 mg-C per mg-Chl per day near the surface. From earlier calculations, the numerator integral in Equation (B-1), taken over a solar day, would be 9.46 times the integral corresponding to the photosynthetically optimal hour only (maximum integrand). The ratio $82/9.46 = 8.66$ mg-C per mg-Chl per hour is consistent with the data of Ondrusek et al. (2001).

NOMENCLATURE

[A]	ammonium concentration (nM)
A_θ	temperature factor in Equation (5)
A_{light}	light factor in Equation (5), described in Equation (6)
A	heat exchanger surface (m^2)
b	plume radius (m)
c_p	specific heat of seawater (J/kg-K)
$[Chl a]$	chlorophyll-a concentration ($\mu\text{g/l}$)
B_o	initial plume buoyancy flux (m^4/s^3)
F	auxiliary function representative of New Production ($\text{mg-C}/\text{m}^3$)
g	acceleration of gravity (m/s^2)
H	heat transfer coefficient ($\text{W}/\text{m}^2\text{-K}$)
h_T	plume neutral-buoyancy (stabilization) depth (m)
GPP	Gross Primary Production ($\text{mg-C}/\text{m}^3\text{-day}$ or equivalent unit)
I	PAR irradiance ($\text{E}/\text{m}^2\text{-s}$)
I_m	constant in Equation (5) for the ammonium inhibition of nitrate uptake
I_{max}	maximum (Noon) PAR irradiance ($\text{E}/\text{m}^2\text{-s}$)
k	temperature coefficient in A_θ (K^{-1})
K	half-saturation constant (nM)
K_i	half-saturation constant for the

TABLE B-1

Values of V inferred from Harrison et al. (1996)^a

Cruise		V_N (day^{-1})	V_A (day^{-1})
CJGOFS-92 (oceanic)	Mean:	0.11	0.89
	Range:	0.02-0.38	0.20-3.39
CJGOFS-93 (oceanic)	Mean:	0.42	1.26
	Range:	0.05-2.06	0.33-5.91
WOCE-93	Mean:	0.35	2.25
	Range:	0.16-1.51	1.22-7.03

^aMean based on means of ρ_m and $[Chl a]$; range defined by low value of ρ_m over high value of $[Chl a]$, high value of ρ_m over low value of $[Chl a]$.

	ammonium inhibition of nitrate uptake (nM)	η	near-field mixing efficiency
M_x	horizontal plume momentum flux (kg-m/s ²)	κ	light extinction coefficient (m ⁻¹)
M_z	vertical plume momentum flux (kg-m/s ²)	λ	wavelength of neutrally-buoyant plume oscillations (m)
N	buoyancy frequency (rad/s)	ϕ	angle of plume trajectory from horizontal
[N]	nitrate (plus nitrite) concentration (nM)	ρ	potential density (kg/m ³)
NP	New Production (mg-C/m ³ -day or equivalent unit)	ρ_m	maximum hourly photosynthetic production in Harrison et al. (1996) (nM-N/h)
q	thermal power in heat exchanger (W)	θ	temperature (°C)
Q	plume volume flow rate (m ³ /s)	τ	plume settling time (s)
s	plume centerline curvilinear coordinate (m)	ξ_{abs}	absolute near-field enhancement index (mg-Chl-a/s)
S	absolute dilution of nutrient-rich deep water ($S \geq 1$)	ξ_{rel}	relative near-field enhancement index
S_{opt}	dilution of deep water with surface water that maximizes the function F/A_{light}	Subscripts	
t	time (hr)	a	ambient values
T	generic notation for plume tracer flux	A	ammonium
U_a	horizontal current (m/s)	N	nitrate
u	plume centerline velocity (m/s)	o	properties of deep upwelled water
V	maximum daily photosynthetic rate (day ⁻¹)	opt	optimum
x	horizontal coordinate (m)	out	properties of seawater leaving a heat exchanger
z	vertical coordinate (m)	ref	reference
X	horizontal plume centerline coordinate (m)	s	properties of surface water
Z	vertical plume centerline coordinate (m)		

Greek letters

α	plume first entrainment coefficient
β	plume second entrainment coefficient
$\Delta\theta_A$	auxiliary temperature difference in heat exchanger calculations (°C)
$\Delta\theta_B$	auxiliary temperature difference in heat exchanger calculations (°C)
$\Delta\theta_{LMTD}$	Logarithmic Mean Temperature Difference (°C)

REFERENCES

- Allen, C. (1994). "New Production and the f-Ratio in a Mesoscale Eddy in the Lee of the Island of Hawai'i," Master's Thesis, Department of Oceanography, University of Hawaii, 130 pages.
- Allen, C. B., Kanda, J. and Laws, E. A. (1996). "New production and photosynthetic rates within and outside a cyclonic mesoscale eddy in the North Pacific subtropical gyre," *Deep Sea Research I*, 43(6), 917-936.
- Bidigare, R. R., Benitez-Nelson, C., Leonard, C. L., Quay, P. D., Parsons, M. L., Foley, D. G. and Seki, M. P. (2003). "Influence of a cyclonic eddy on microheterotroph biomass and carbon export in the lee of Hawaii," *Geophysical Research Letters*, 30(6), 4 pages.

- Bidigare, R. R. (February 5, 2005). personal communication.
- Fischer, H. B., List, E. J., Koh, R. C. Y., Imberger, J. and Brooks, N. H., *Mixing in Inland and Coastal Waters*, Academic Press, New York, 483 pages.
- Flament, P., Kennan, S., Lumpkin, R., Sawyer, M. and Stroup, E. D. (1996). "The Ocean Atlas of Hawaii," <http://www.satlab.hawaii.edu/atlas/>, Department of Oceanography, School of Ocean and Earth Science and Technology, University of Hawaii.
- Fofonoff, P. and Millard Jr., R. C. (1983). "Algorithms for computation of fundamental properties of seawater," *UNESCO Technical Papers in Marine Sciences*, **44**, 53 pages.
- Fujieki, L. A., Santiago-Mandujano, F., Sheridan, C., Lukas, R., Karl, D. and other contributors (October 2004). "Hawaii Ocean Time-series – Data Report 13: 2001," http://hahana.soest.hawaii.edu/hot/reports/rep_y13.pdf, 270 pages.
- Harrison, W.G., Harris, L. R. and Irwin, B. D. (1996). "The kinetics of nitrogen utilization in the oceanic mixed layer: Nitrate and ammonium interactions at nanomolar concentrations," *Limnology and Oceanography*, **41**(1), 16-32.
- Hewett, T. A., Fay, J. A. and Hoult, D. P. (1971). "Laboratory experiments of smokestack plumes in a stable atmosphere," *Atmospheric Environment*, **5**, 767-789.
- Hoult, D. P., Fay, J. A. and Forney, L. J. (1969). "A theory of plume rise compared with field observations," *Journal of the Air Pollution Control Association*, **19**, 585-590.
- Huang, H., Fergen, R. E., Proni, J. R. and Tsai, J. J. (1998). "Initial dilution equations for buoyancy-dominated jets in current," *ASCE Journal of Hydraulic Engineering*, **124**(1), 105-108.
- Kajikawa, T. (1997). "Increasing productivity by utilization of deep ocean water: field and experimental investigation in Japan," *Proceedings of the NSF Workshop on Engineering Research Needs for Off-Shore Mariculture Systems*, 447-472.
- Karl, D. M. and Lukas, R. (1996). "The Hawaii Ocean Time-series (HOT) program: Background, rationale and field implementation," *Deep Sea Research II*, **43**(2-3), 129-156.
- Kawamiya, M., Kishi, M. J., Yamanaka, Y. and Sugiharara, M. (1995). "An ecological-physical coupled model applied to Station Papa," *Journal of Oceanography*, **51**, 635-664.
- Kishi, M. J., Motono, H., Kashiwai, M. and Tsuda, A. (2001). "An ecological-physical coupled model with ontogenetic vertical migration of zooplankton in the Northwestern Pacific," *Journal of Oceanography*, **57**, 499-507.
- Kreith, F., and M. S. Bohn (1973). *Principles of Heat Transfer*, 5th edition, West Publishing Company, St Paul, MN, 720 pages.
- Liu, C. C. K., Sou, I. M. and Huashan, L. (2003). "Artificial Upwelling and Near-field Mixing of Deep-ocean Water Effluent," *Journal of Marine Environmental Engineering*, **7**, 1-14.
- Menesguen A., Monbet, Y. and Cousin, F. (1989). "OTEC's subsurface discharges of deep ocean water: modeling their effects on the primary production," *Proc. ASCE International Conference on Ocean Energy Recovery*, 235-246, 1989.
- Morton, B. R., Taylor, G. I. and Turner, J. S. (1956). "Turbulent gravitational convection from maintained and instantaneous sources," *Proceedings of the Royal Society of London*, **A234**, 1-23.
- Nihous, G.C., Tang, L. and Masutani, S. M. (2003). "A sinking plume model for deep CO₂ discharge," *Proc. GHGT-6 Conference*, J. Gale and Y. Kaya (editors), Elsevier Science, Oxford, 765-770.
- Ondrusek, M. E., Bidigare, R. R., Waters, K. and Karl, D. M. (2001). "A predictive model for estimating rates of primary production in the subtropical North Pacific Ocean," *Deep Sea Research II*, **48**(8-9), 1837-1863.
- Ouchi, K. and Ohmura, H. (2004). "The design concept and experiment of ocean nutrient enhancer TAKUMI," *Proc. Oceans '04/Techno-Oceans '04*, 6 pages.
- Platt, T., Gallegos, C. L. and Harrison, W. G. (1980). "Photoinhibition of photosynthesis in natural assemblages of marine phytoplankton," *Journal of Marine Research*, **38**(4), 687-701.
- Siegel, D. A., Karl, D. M. and Michaels, A. F. Guest Editors (2001). "HOT and BATS: interpretations of open ocean biogeochemical processes," *Deep Sea Research II*, **48**(8-9), 1403-2105.
- Stommel, H., Arons, A. B., and D. Blanchard (1956). "An oceanographic curiosity: the perpetual salt fountain," *Deep Sea Research*, **3**(2), 152-153.
- Takahashi, P. K., McKinley, K. R., Phillips, V. D., Magaard, L. and Koske, P. (1993). "Marine macrobiotechnology systems," *Journal of Marine Biotechnology*, **1**, 9-15.
- Vaillancourt, R. D., Marra, J., Seki, M. P., Parsons, M. L. and Bidigare, R. R. (2003). "Impact of a cyclonic eddy on phytoplankton community structure and photosynthetic competency in the subtropical North Pacific Ocean," *Deep Sea Research I*, **50**, 829-847.
- Vaulot, D. (2001). "Phytoplankton," Article in *Encyclopedia of Life Sciences*, Macmillan Publishers Ltd., Nature Publishing Group, 1-7.
- Wozniak, B., Dera, J., Ficek, D., Ostrowska, M. and Majchrowski, R. (2002). "Dependence of the photosynthesis quantum yield in oceans on environmental factors", *Oceanologia*, **44**(4), 439-459.
- Wright, S. J. (1977). "Mean behavior of buoyant jets in a crossflow," *ASCE Journal of the Hydraulics Division*, 499-513.
- Yanagi, T., Onitsuka, G., Hirose, N. and Yoon, J. H. (2001). "A numerical simulation on the mesoscale dynamics of the Spring bloom in the Sea of Japan," *Journal of Oceanography*, **57**, 617-630.